

## Article

# Research on the Spatial-Temporal Patterns of Carbon Effects and Carbon-Emission Reduction Strategies for Farmland in China

Ying Wang <sup>1,2,\*</sup>, Juan Yang <sup>1</sup> and Caiquan Duan <sup>1</sup> <sup>1</sup> College of Engineering, Northeast Agricultural University, Harbin 150030, China<sup>2</sup> Key Laboratory of Combining Farming and Animal Husbandry, Ministry of Agriculture and Rural Affairs, Harbin 150086, China

\* Correspondence: yingwang@neau.edu.cn

**Abstract:** Agriculture has the dual effects of serving as a carbon source and uptaking carbon. Studying the carbon effects of agriculture has great theoretical and practical importance. Based on China's provincial panel data from 2007 to 2020, using the life cycle method, this paper studied the carbon effects of farmland in China from the perspective of carbon sources and uptake. The spatiotemporal distribution characteristics of carbon effects were analysed, and the carbon-emission reduction potential was calculated. The results displayed that the carbon emissions from farmland in China had a fluctuating downwards trend from 2007 to 2020, with the highest carbon emissions in 2013. The carbon-emission intensity generally displayed a downwards trend, exhibiting a "cold north and hot south" spatial pattern. Furthermore, carbon uptake displayed an overall upwards trend during the study period, increasing by 27.73% compared to that in 2007. Rice, maize, and wheat were the main sources of carbon uptake, and high-carbon-uptake areas were mainly distributed in eastern China; conversely, low-carbon-uptake areas were mainly distributed in southwestern China. Chinese farmland mainly served as net carbon-uptake areas, increasing from  $522.81 \times 10^6$  t in 2007 to  $734.50 \times 10^6$  t in 2020. Notably, there were significant differences in net carbon uptake among 31 provinces in China, with a prominent polarization phenomenon. China has great potential for reducing carbon emissions from farmland. Finally, based on the results of clustering carbon-emissions reduction potential, differentiated agricultural management strategies were developed to provide a reference and solutions for decision making related to agricultural "dual-carbon" strategies.

**Keywords:** carbon emissions; carbon uptakes; carbon effect; carbon-emissions reduction strategies; farmland



check for updates

**Citation:** Wang, Y.; Yang, J.; Duan, C. Research on the Spatial-Temporal Patterns of Carbon Effects and Carbon-Emission Reduction Strategies for Farmland in China. *Sustainability* **2023**, *15*, 10314. <https://doi.org/10.3390/su151310314>

Academic Editors: Manuela Vaz Velho, Ana Pinto de Moura, Edgar Pinto and Manuela Vieira da Silva

Received: 17 May 2023  
Revised: 19 June 2023  
Accepted: 26 June 2023  
Published: 29 June 2023



**Copyright:** © 2023 by the authors. Licensee MDPI, Basel, Switzerland. This article is an open access article distributed under the terms and conditions of the Creative Commons Attribution (CC BY) license (<https://creativecommons.org/licenses/by/4.0/>).

## 1. Introduction

Global climate change, characterized by global warming, is one of the environmental problems humans currently face and it has already threatened human survival and the sustainable development of ecosystems [1]. In the face of such unfavourable circumstances, countries around the world have proposed voluntary actions. In September 2020, President Xi Jinping announced China's goal of reaching its peak carbon-dioxide emissions before 2030 and achieving carbon neutrality by 2060 (i.e., the "dual-carbon" goal) [2]. Farmland is a significant source of greenhouse gas emissions, and the Sixth Assessment Report of the Intergovernmental Panel on Climate Change (IPCC) shows that global agricultural and forestry emissions account for 23% of all anthropogenic greenhouse gas emissions [3]. China is a major agricultural country, and its agricultural greenhouse gas emissions account for 17% of the country's total greenhouse gas emissions [4]. Therefore, studying carbon sources and carbon uptake in agriculture will help accelerate the process of achieving carbon peaking and implementing carbon neutrality strategies, which have important strategic significance and practical value for China's "dual-carbon" goal.

Farmland has the dual effects of serving as a carbon source and uptaking carbon. The carbon emissions from farmland mainly come from energy consumption, agricultural production inputs, rice cultivation, straw burning, and soil. In terms of the composition of the emissions,  $N_2O$ ,  $CH_4$ , and  $CO_2$  are the main greenhouse gases emitted from farmland. Regarding the calculation of carbon emissions from farmland, given the limitations related to manpower, material resources, and technology, the current method used is the IPCC approach, which classifies agricultural production activities based on different input factors and calculates the total emissions [5]. Farmland absorbs greenhouse gases through crop photosynthesis and soil carbon uptake. Compared with that on carbon uptake in farmland soil, research on farmland crop carbon uptake is relatively weak. Crop carbon uptake in agricultural production systems is generally less than soil carbon uptake. However, within a certain regional range, the amount of crop carbon uptake is still considerable and has the potential to increase [6]. The methods for estimating crop carbon uptakes mainly include parameter estimations [7], remote sensing simulations [8], and model simulations based on physiological and ecological processes [9,10].

To achieve the “dual-carbon” goal, scholars have conducted systematic research on the carbon effects of farmland. Currently, the research mainly focuses on the following areas: (1) estimation and analysis of carbon emissions and carbon uptake on farmland at the national or regional level, such as Dioha estimated the total greenhouse gas emissions from the Nigerian agriculture sector [11], Hemingway estimated the greenhouse gas emissions from crops in an Indian village [12], Li calculated the carbon emissions and carbon uptakes on the Qinghai–Tibet Plateau in China [13], and Dyer assessed energy-based greenhouse gas emissions from Canadian agriculture [14]; (2) factors influencing carbon effects on farmland, such as agricultural inputs [15,16], land-use changes [17,18], planting and cultivation patterns [19,20], and straw return [21], and driving mechanisms of carbon emissions in farmland, including agricultural technology [22], national policies [23], and markets [24]; (3) predictions of carbon emissions by grey prediction models [25,26], neural networks [27,28], the STIRPAT model [29], and estimations of carbon-emissions reduction potential [30]; and (4) carbon-uptake enhancement and emissions-reduction pathways and policies, including integrated crop–livestock systems [31], organic farming [32], conservation tillage [33,34], intermittent water-saving irrigation, agricultural investments [35], and a series of policy recommendations [36].

At present, although there have been many important achievements related to studying farmland carbon effects, there are still some issues that need further research. First, research on farmland carbon uptake, especially net carbon uptake, is not sufficient. Net carbon uptake can closely link carbon uptake with carbon sources, which is an important prerequisite and foundation for an in-depth study of the carbon effects on farmland. Second, research on the carbon-emission reduction potential of farmland is mostly focused on the comparison of emission reduction potential among provinces and the impact of emission reduction measures. However, when exploring the differences in carbon-emission reduction potential among provinces, existing studies have only used simple geographical divisions and have not comprehensively considered the differences in agricultural production in different regions.

Based on the above issues, this study applies an improved carbon-emission coefficient method [37], which can comprehensively measure the emissions of  $CO_2$ ,  $CH_4$ , and  $N_2O$  from farmland, and a crop-growth period carbon-uptake measurement model to calculate the total greenhouse gas emissions (referred to as carbon emissions in this paper), carbon uptake, and net carbon uptake on Chinese farmland. Using convergence theory and the parameter-comparison method, this study estimates carbon-emission reduction potentials in different regions of China. The main objectives of this study are (1) to clarify the spatial-temporal characteristics and patterns of carbon emissions and carbon uptake on Chinese farmland, quantify the net carbon-uptake level on Chinese farmland from 2007 to 2020, and (2) explore the carbon-emissions reduction potential of Chinese farmland. The study aims to provide basic data support and a decision making basis for the government to make

decisions on the agricultural “dual-carbon” goal and help achieve low-carbon, sustainable, and high-quality agriculture.

The rest of the paper is divided into four sections. Section 2 describes the data sources and research methodology. Section 3 provides the spatial and temporal evolution of carbon emissions, carbon uptake, and net carbon uptake; the potential for carbon-emissions reduction on farmland; and differentiated management measures. Section 4 contains further discussion, limitations, and prospects. Section 5 concludes with our findings.

## 2. Materials and Methods

### 2.1. Data Sources

Using national statistical data, this study obtained data on agricultural inputs, irrigated land area, cultivated land area, crop yields, rice sowing area, agricultural output value, and other data from 2007 to 2020. Considering the availability of crop yield data, this study only selected 13 major crops, rice, wheat, maize, bean, potato, cotton, rapeseed, peanuts, sesame, hemp, sugarcane, sugar beet, and tobacco, to calculate the carbon emissions and carbon uptake on Chinese farmland. Using the above data, this study calculated the carbon emissions, carbon-emission intensity, and carbon uptake on farmland in 31 provinces of China, excluding Taiwan, Macao, and Hong Kong special administrative regions, and then calculated net carbon uptake. These data were used to evaluate the carbon effect of Chinese farmland, as shown in Figure 1.

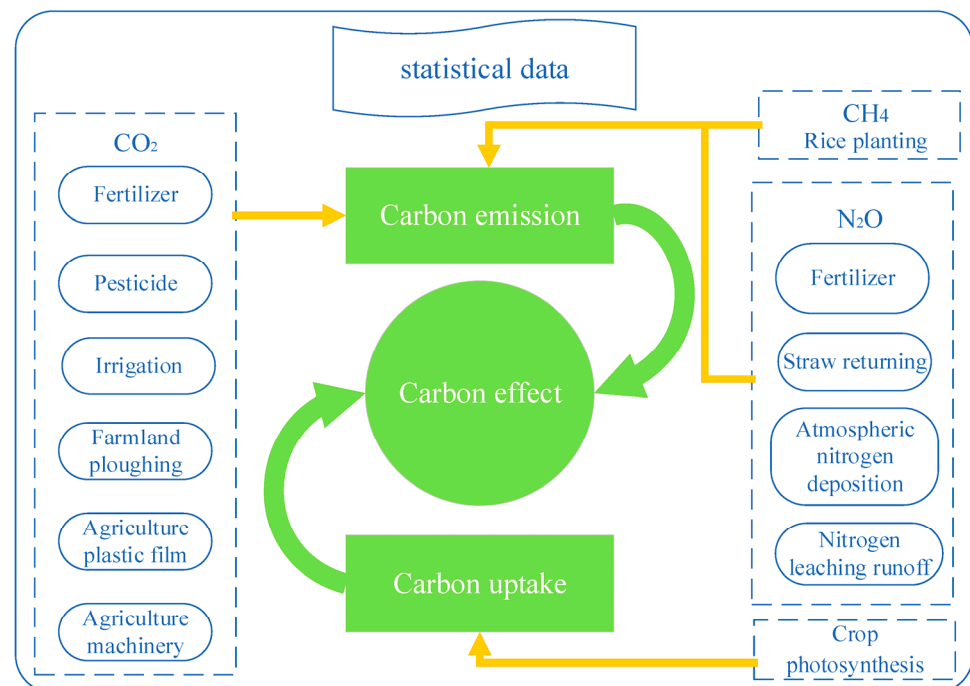


**Figure 1.** Assessment of the carbon effect on Chinese farmland.

### 2.2. Farmland Carbon Effect Assessment Method

#### 2.2.1. Calculation of Farmland Carbon Emissions

This study converted three greenhouse gases into CO<sub>2</sub> equivalents based on their respective warming potentials and calculates the total carbon emissions. Among them, CO<sub>2</sub> emissions mainly originate from agricultural inputs. This study calculated CO<sub>2</sub> emissions from agricultural irrigation, tillage, machinery use, pesticide use, agricultural film use, and fertilizer application. The calculation formula is as follows:

$$E_{CO_2} = \sum_{j=1}^n T_j \times EF_j \times 44/12 \quad (1)$$

where  $E_{CO_2}$  is the CO<sub>2</sub> emissions (kg),  $T_j$  represents the amount of the  $j$ -type of agricultural input (kg),  $EF_j$  represents the carbon-emission coefficient of the  $j$ -type of agricultural input, and 44/12 is the ratio of molecular weight of CO<sub>2</sub> to C. The carbon-emission coefficients for the different agricultural inputs are shown in Table 1.

**Table 1.** Carbon-emission coefficients of agricultural production activities.

Carbon-Emission Pathway	Carbon-Emission Coefficient	Reference Sources
Phosphate fertilizer	0.200 g/g	[37]
Potash fertilizer	0.150 g/g	[37]
Diesel	0.597 g/g	[38]
Irrigation	266.480 kg/hm <sup>2</sup>	[39]
Ploughing	3.126 kg/hm <sup>2</sup>	[40]
Agricultural film	5.180 g/g	[41]
Pesticide	4.934 g/g	[42,43]

CH<sub>4</sub> emissions from farmland are mainly from rice cultivation. CH<sub>4</sub> emissions expressed in CO<sub>2</sub> equivalents were calculated as follows:

$$E_{CH_4} = \sum EF_i \times AD_i \times 25 \quad (2)$$

where  $E_{CH_4}$  is the CH<sub>4</sub> emissions expressed in CO<sub>2</sub> equivalents (kg);  $EF_i$  represents the CH<sub>4</sub> emission factor of rice fields (kg/hm<sup>2</sup>), with  $i$  representing the type of rice field;  $AD_i$  represents the corresponding rice-planting area for the emission factor (hm<sup>2</sup>); and 25 represents the warming potential of CH<sub>4</sub> [38].

The main sources of N<sub>2</sub>O emissions are direct nitrogen emissions caused by straw return and fertilizer application, as well as indirect nitrogen emissions caused by nitrogen leaching and runoff from fields and atmospheric nitrogen deposition. N<sub>2</sub>O emissions expressed in CO<sub>2</sub> equivalents were calculated as follows:

$$E_{N_2O} = (N_z + N_j) \times 44/28 \times 298 \quad (3)$$

where  $E_{N_2O}$  is the N<sub>2</sub>O emissions expressed in CO<sub>2</sub> equivalents (kg),  $N_z$  represents direct nitrogen emissions (kg),  $N_j$  represents indirect nitrogen emissions (kg), 44/28 is the ratio of molecular weight of N<sub>2</sub>O to N, and 298 is the warming potential of N<sub>2</sub>O [38]. The calculation method for  $N_z$  is as follows:

$$N_z = (N_h + N_g) \times EF_z \quad (4)$$

where  $N_h$  is the amount of nitrogen applied by chemical fertilizer (kg), the amount of nitrogen in compound fertilizer is calculated as 1/3 of its total weight [37],  $N_g$  represents the total amount of nitrogen in straw returned to the field (kg), and  $EF_z$  represents the direct emission factor of N<sub>2</sub>O.

The calculation method for  $N_g$  is as follows:

$$N_g = \sum_{i=1}^n (M_i/L_i - M_i) \times \beta_i \times K_i + M_i/L_i \times \alpha_i \times K_i \quad (5)$$

where  $M_i$  is the grain yield of crop  $i$ ,  $L_i$  is the economic coefficient of crop  $i$ , and  $\beta_i$  is the straw-return rate of crop  $i$ . As there are no statistical data on straw-return rates in different provinces, a uniform rate of 0.2 is used in this study [37].  $K_i$  represents the nitrogen content in straw of crop  $i$ , and  $\alpha_i$  is the root-to-crown ratio of crop  $i$ . The parameters are shown in Table 2 [44].

**Table 2.** Main crop parameters.

Crop Type	Nitrogen Content in Straw	Economic Coefficient	Root-to-Crown Ratio	Carbon Absorption Rate	Moisture Content
Rice	0.00753	0.489	0.125	0.414	0.12
Wheat	0.00516	0.434	0.166	0.485	0.12
Maize	0.00580	0.438	0.170	0.471	0.13
Bean	0.02005	0.405	0.130	0.450	0.13
Potato	0.01100	0.667	0.050	0.423	0.70
Cotton	0.00548	0.383	0.200	0.450	0.08
Rapeseed	0.00548	0.271	0.150	0.450	0.10
Peanut	0.01820	0.556	0.200	0.450	0.10
Sesame	0.01310	0.417	0.200	0.450	0.15
Hemp	0.01310	0.830	0.200	0.450	0.15
Sugarcane	0.83000	0.750	0.260	0.450	0.50
Beet	0.00507	0.667	0.050	0.407	0.75
Tobacco	0.01440	0.830	0.200	0.450	0.85

The calculation method for  $N_j$  is as follows:

$$N_j = (N_h + N_g) \times 0.0025 \quad (6)$$

The formulas for calculating the total amount and intensity of carbon emissions from farmland are as follows:

$$E = E_{CO_2} + E_{CH_4} + E_{N_2O} \quad (7)$$

$$EI = E / GDP_A \quad (8)$$

where  $E$  is the farmland carbon emissions (kg),  $EI$  represents the carbon-emission intensity (kg/CNY), and  $GDP_A$  represents agricultural output value (CNY).

### 2.2.2. Calculation of Farmland Carbon Uptake

Considering the data availability, the carbon uptake in farmland soil was not calculated. This study only estimated the carbon uptakes of crops on farmland, which refers to the carbon absorbed through photosynthesis during the crop-growth period, estimated based on crop yield, economic coefficient, and carbon-absorption rate [45]. The formula is as follows:

$$C_t = \sum_{i=1}^n C_d = \sum_{i=1}^n [C_i \times M_i \times (1 - W_i) \times (1 + \alpha_i)] / L_i \quad (9)$$

where  $C_t$  is the carbon uptake of farmland;  $i$  represents the  $i$ -type crop;  $C_d$  represents the amount of carbon absorbed by a certain crop during its entire growth period;  $C_i$  represents the carbon absorbed by a unit of synthesized organic matter (dry weight) during the entire growth period of crop  $i$ , which is the carbon absorption rate; and  $W_i$  represents the moisture content of the harvested part of crop  $i$ . The parameters are shown in Table 2.

### 2.3. Spatial Autocorrelation

Spatial autocorrelation is a method of spatial data analysis that mainly investigates whether observations at one location in space are related with the observations at neighbouring locations, including global spatial autocorrelation and local spatial autocorrelation [46]. Global spatial autocorrelation describes the spatial characteristics of variables over an entire area and can accurately analyse the overall spatial correlation characteristics. Local spatial autocorrelation analysis is the characterization of local spatial heterogeneity and the identification of “hot spot” and “cold spot” in different spatial locations [47].

Moran's  $I$  index was employed to reflect the overall spatial pattern of carbon emissions from Chinese farmland. The calculation formula is as follows:

$$I = \frac{n \sum_{i=1}^n \sum_{j=1}^n W_{ij} (X_i - \bar{X})(X_j - \bar{X})}{\sum_{i=1}^n \sum_{j=1}^n W_{ij} \sum_{i=1}^n (X_j - \bar{X})^2} \quad (10)$$

where  $I$  is the global Moran's index,  $n$  represents the number of provinces,  $X_i$  represents the carbon-emission intensity of the  $i$ -type province,  $W_{ij}$  represents the weight between spatial units  $i$  and  $j$ , and  $\bar{X}$  represents the average carbon-emission intensity of the study areas.

Getis Ord ( $G_i^*$ ) measures the density of high value (hot spot) and low value (cold spot) in a given study area, and is calculated as follows:

$$G_i^* = \frac{\sum_{j=1}^n w_{ij} x_j - \bar{X} \sum_{j=1}^n w_{ij}}{S \sqrt{\left[ n \sum_{j=1}^n w_{ij}^2 - \left( \sum_{j=1}^n w_{ij} \right)^2 \right] / (n-1)}} \quad (11)$$

$$S = \sqrt{\frac{1}{n} \sum_{j=1}^n x_j^2 - \bar{X}^2} \quad (12)$$

where  $G_i^*$  is the local spatial autocorrelation index. A high value of  $G_i^*$  indicates that adjacent areas have high-value clusters, which are hot spots. A low value of  $G_i^*$  indicates that adjacent areas have low-value clusters, which are cold spots. A value of  $G_i^*$  trending towards 0 indicates the absence of the clustering phenomenon.

#### 2.4. Parameter-Comparison Method

Carbon-emissions reduction potential refers to whether carbon emissions can be reduced and how much the maximum amount of carbon emissions can be reduced, which is a relative value. Therefore, in this study, a parameter-comparison method was adopted to determine the size of the carbon-emission reduction potential. One benchmark was selected in advance to compare the existing carbon-emission levels in each region with the benchmark, and, then, the difference between them was the carbon-emission reduction potential. The key to this method lies in the measurement of the carbon emissions. Referring to a previous study [48], carbon-emission intensity was used to measure the level of carbon emissions from agriculture. The carbon-emissions reduction potential is calculated as follows:

$$P_i = 1 - EI_{\min} / EI_i \quad (13)$$

where  $P_i$  is the carbon-emissions reduction potential of province  $i$ ,  $EI_{\min}$  represents the minimum value of carbon-emission intensity, and  $EI_i$  represents the carbon-emission intensity of province  $i$ .

### 3. Results

#### 3.1. Temporal and Spatial Changes in Carbon Emissions from Farmland

China's farmland carbon emissions displayed a fluctuating downwards trend from 2007 to 2020. The carbon emissions decreased from  $8.5321 \times 10^8$  t to  $8.4511 \times 10^8$  t, reaching a peak in 2013 at  $9.4665 \times 10^8$  t (Figure 2). The development trend of farmland carbon emissions in China can be generally divided into four stages: a period of rapid growth from 2007 to 2008, during which China's farmland carbon emissions increased rapidly from  $8.5321 \times 10^8$  t in 2007 to  $8.9094 \times 10^8$  t in 2008, with an average annual growth rate of 4.42% and an average increase of  $0.3773 \times 10^8$  t per year; a slow decrease stage for the years 2007–2008, during which China's farmland carbon emissions decreased slowly from  $8.9094 \times 10^8$  t in 2008 to  $8.7077 \times 10^8$  t in 2010, with an average annual decrease rate of

1.14% and an average decrease of  $0.1009 \times 10^8$  t per year; a period of rapid growth from 2010 to 2013, during which China's farmland carbon emissions rapidly increased from  $8.7086 \times 10^8$  t in 2010 to  $9.4665 \times 10^8$  t in 2013, with an average annual growth rate of 2.83% and an average increase of  $0.2530 \times 10^8$  t per year; and then a continuous decline stage in the period of 2003–2020, during which China's farmland carbon emissions continued to decline from  $9.4665 \times 10^8$  t in 2013 to  $8.4511 \times 10^8$  t in 2020, with an average annual decrease rate of 1.53% and an average decrease of  $0.1451 \times 10^8$  t per year, indicating a significant and sustained reduction. From the point of view of the structure of carbon emissions in farmland,  $N_2O$ ,  $CH_4$ , and  $CO_2$  accounted for 59.34%, 18.05%, and 22.61% of the total carbon emissions, respectively. From 2007 to 2020, only  $N_2O$  emissions decreased, while the total emissions of the other two greenhouse gases displayed a slight increase.

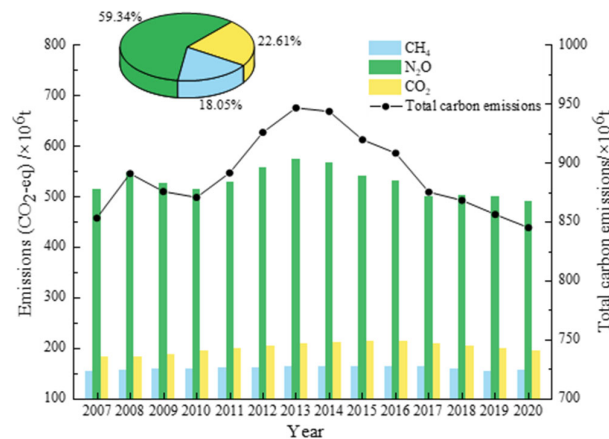


**Figure 2.** Carbon emissions from farmland in China.

In addition, the carbon-emission intensity of farmland, which is the carbon emissions per unit of agricultural output, was calculated. The carbon-emission intensity of Chinese farmland displayed a downwards trend (Figure 3). The changes in total carbon emissions and agricultural production value directly affect the changes in carbon-emission intensity. The mean carbon-emission intensity decreased from 0.339 kg/CNY in 2007 to 0.107 kg/CNY in 2020, with an average annual decrease of 0.017 kg/CNY. Its development trend can be generally divided into three stages: a significant decrease stage from 2007 to 2009, where the annual average decrease rate was 8.85%; a large decrease stage in 2009–2011, where the annual average decrease rate was 13.81%; and a slow decrease stage in 2011–2020, where the annual average decrease rate was 7.20%, accompanied by a slow increase in China's agricultural output and a reduction of total carbon emissions.

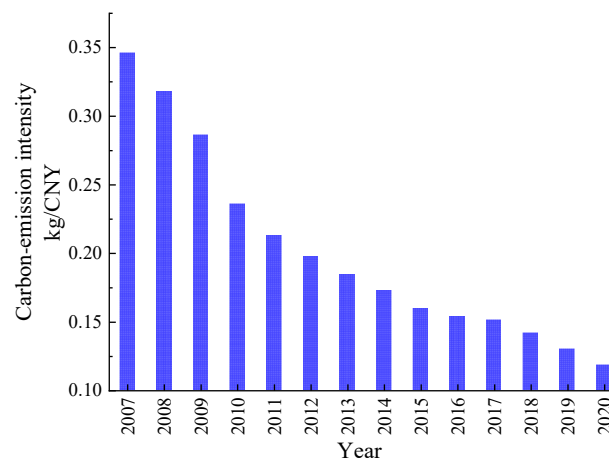


**Figure 3.** Carbon-emission intensity of farmland in China.

The global spatial autocorrelation Moran's  $I$  index and significance levels ( $Z$  score and  $p$  value) of the carbon-emission intensity in Chinese farmland for 2007, 2010, 2015, and 2020 were obtained (Table 3). The global spatial autocorrelation index  $I$  values of farmland carbon emissions in different years were positive and passed the 5% significance test, indicating that the carbon-emission intensity of farmland in different provinces in China had a positive spatial correlation. Moran's  $I$  value increased and then decreased, indicating that the degree of spatial clustering of provinces with similar farmland carbon-emission intensities in China first increased to a certain extent and then decreased to a certain extent, but, overall, it was in a clustered state spatially.

**Table 3.** Global spatial autocorrelation index and its significance levels for China's farmland in 2007, 2010, 2015, and 2020.

Parameter	2007	2010	2015	2020
$I$	0.146081	0.181396	0.149956	0.125180
$Z$	2.778227	3.310540	3.215307	2.887993
$P$	0.005466	0.000931	0.001303	0.003877

The spatial autocorrelation index Getis–Ord ( $G_i^*$ ) was calculated for each province in 2007, 2010, 2015, and 2020, and they were divided into four levels according to the natural breaks method, from high to low, as follows: hot spot area, subhot spot area, subcold spot area, and cold spot area. Then, the spatial pattern evolution maps of Chinese farmland carbon-emission intensity for the four time points were drawn, as shown in Figure 4.

From the perspective of the overall spatial structure, the overall pattern of carbon-emission intensity hot spots in Chinese farmland remained stable, displaying a spatial pattern of “cold north and hot south”. Guizhou, Yunnan, Guangdong, Guangxi, and Hainan had higher levels of carbon-emission intensity, while Inner Mongolia, Beijing, Tianjin, Ningxia, Shandong, Hebei, Henan, Shanxi, and Shaanxi had lower levels of carbon-emission intensity.

From a regional perspective, the carbon-emission intensity of farmland in the Yangtze River Basin was significantly higher than that in the Yellow River Basin. The climate in the Yangtze River Basin was superior to that in the Yellow River Basin, with significantly better water and heat conditions in the south, making it a suitable area for planting rice and resulting in higher carbon-emission intensity.

In terms of spatial distribution, the overall pattern of carbon-emission intensity in Chinese farmland has remained stable, but some changes have occurred in different types of regions. Between 2007 and 2020, the proportion of hot spot areas for carbon-emission intensity in Chinese farmland increased from 16.13% in 2007 to 32.26% in 2015 and then decreased to 29.03% in 2020. The proportion of subhot areas decreased from 19.35% in 2007 to 12.90% in 2020. The proportion of cold spot areas decreased from 38.71% in 2007 to 32.26% in 2020. The proportion of subcold areas displayed a fluctuating trend, increasing from 25.81% in 2007 to 29.03% in 2010, then decreasing to 22.58% in 2015, and rising again to 25.81% in 2020. Among the four representative years, there were 18 provinces that did not undergo any changes, accounting for 58.06% of the total, indicating that the general pattern of carbon-emission intensity on Chinese farmland has remained unchanged since 2007, with the northern regions mainly having lower values and the southern regions mainly having higher values.

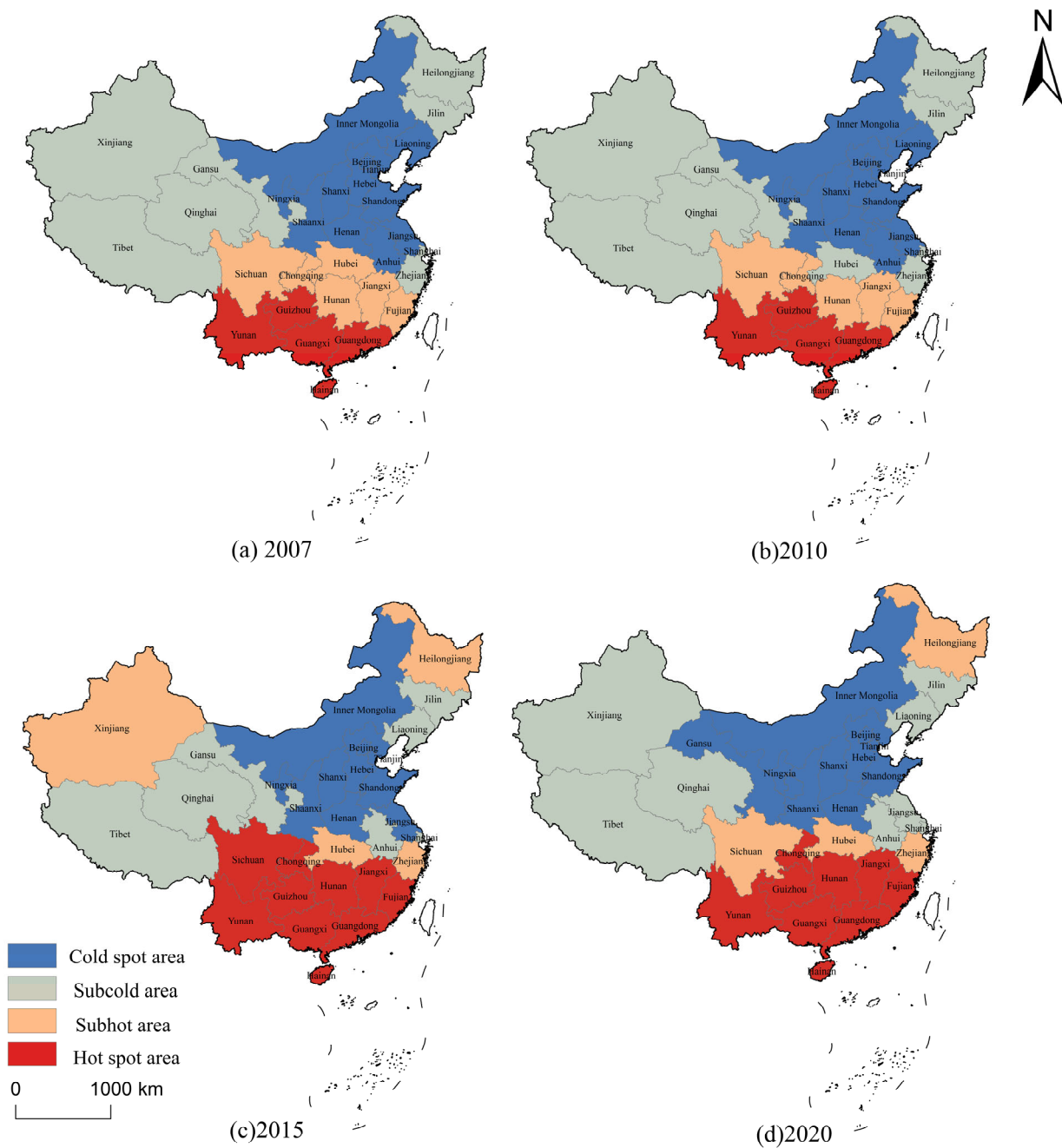


**Figure 4.** Evolution map of carbon-emission intensity hot spots of China's farmland in 2007 (a), 2010 (b), 2015 (c), and 2020 (d).

### 3.2. Temporal and Spatial Changes in Carbon Uptake on Farmland

From 2007 to 2020, the overall carbon uptake on farmland displayed an upwards trend (Figure 5), increasing from  $7.5550 \times 10^8$  t in 2007 to  $9.6503 \times 10^8$  t in 2020, with an average annual growth rate of 1.98%. In this study, crops were divided into wheat, rice, maize, sugarcane, bean, cotton, and other crops. Except for cotton and sugarcane, the carbon uptake of other crops displayed a fluctuating upwards trend. Among them, maize had the largest change in carbon uptakes, increasing by 71.15%. In terms of carbon-uptake composition, rice, maize, and wheat were the main sources of farmland carbon uptake, accounting for 30%, 29%, and 21% of the total carbon uptake, respectively.

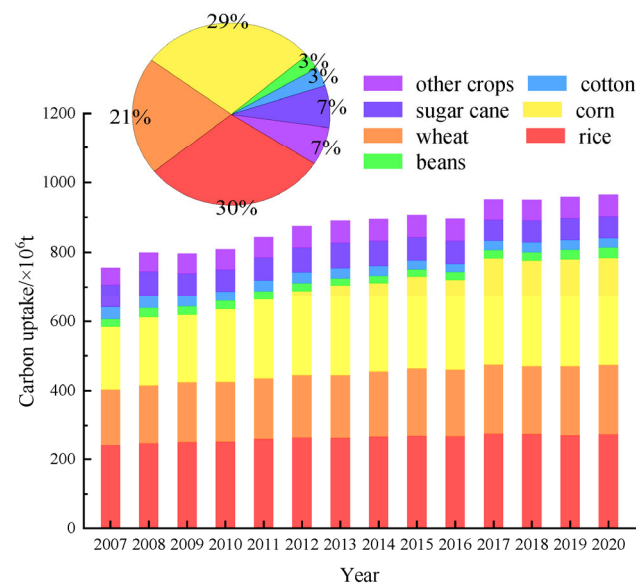


**Figure 5.** Carbon uptake on farmland in China.

There was a visible spatial difference in carbon uptake on Chinese farmland from 2007 to 2020 (Figure 6). The high-carbon-uptake areas were mainly located in eastern China, including Heilongjiang, Shandong, Henan, and Guangxi, accounting for 8.59%, 7.86%, 10.45%, and 6.78% of the total carbon uptake on Chinese farmland, respectively. At the same time, the number of high-carbon-uptake areas gradually increased. The carbon uptake in Xinjiang, Inner Mongolia, Sichuan, Hubei, and Hunan has been increasing, changing from low carbon uptake to high carbon uptake. Due to geographical factors, Tibet and Qinghai have always been in the low-carbon-uptake area. In 2007–2016, Tibet had the lowest amount of carbon uptake on farmland, accounting for only 0.06% of the total amount in China. Beijing had the lowest amount of carbon uptake on farmland, accounting for only 0.04% of the total in China from 2016 to 2020. In 2007–2020, except for that in Beijing, Shanghai, Zhejiang, Fujian, Guangxi, Hainan, Guizhou, Tibet, and Qinghai, the carbon uptake in other provinces increased. Inner Mongolia had the largest increase, with an average annual increase of  $156.34 \times 10^8$  t, while Hainan had the largest decrease, with an average annual decrease of  $13.71 \times 10^8$  t.

### 3.3. Temporal and Spatial Changes in Net Carbon Uptake in Farmland

From the perspective of temporal changes, it was found that China's farmland experienced net carbon uptake for 14 years. As shown in Figure 7, the overall net carbon uptake on China's farmland has been increasing, from  $522.81 \times 10^6$  t in 2007 to  $734.50 \times 10^6$  t in 2020, an increase of 40.49%, with an average annual increase of  $15.12 \times 10^6$  t. Based on the resource endowments of grain production, regional comparative advantages, and consumption characteristics, China has divided 31 provinces into main grain production areas, main grain sales areas, and grain production–sales balance areas. Among them, 13 main grain production areas exist, and they are Hebei, Inner Mongolia, Liaoning, Jilin, Heilongjiang, Jiangsu, Anhui, Jiangxi, Shandong, Henan, Hubei, Hunan, and Sichuan; 7 main grain sales areas exist, and they are Beijing, Tianjin, Shanghai, Zhejiang, Fujian, Guangdong, and Hainan; and 11 grain production–sales balance areas exist, and they are Shanxi, Guangxi, Chongqing, Guizhou, Yunnan, Shaanxi, Qinghai, Ningxia, Xinjiang, Gansu, and Tibet.

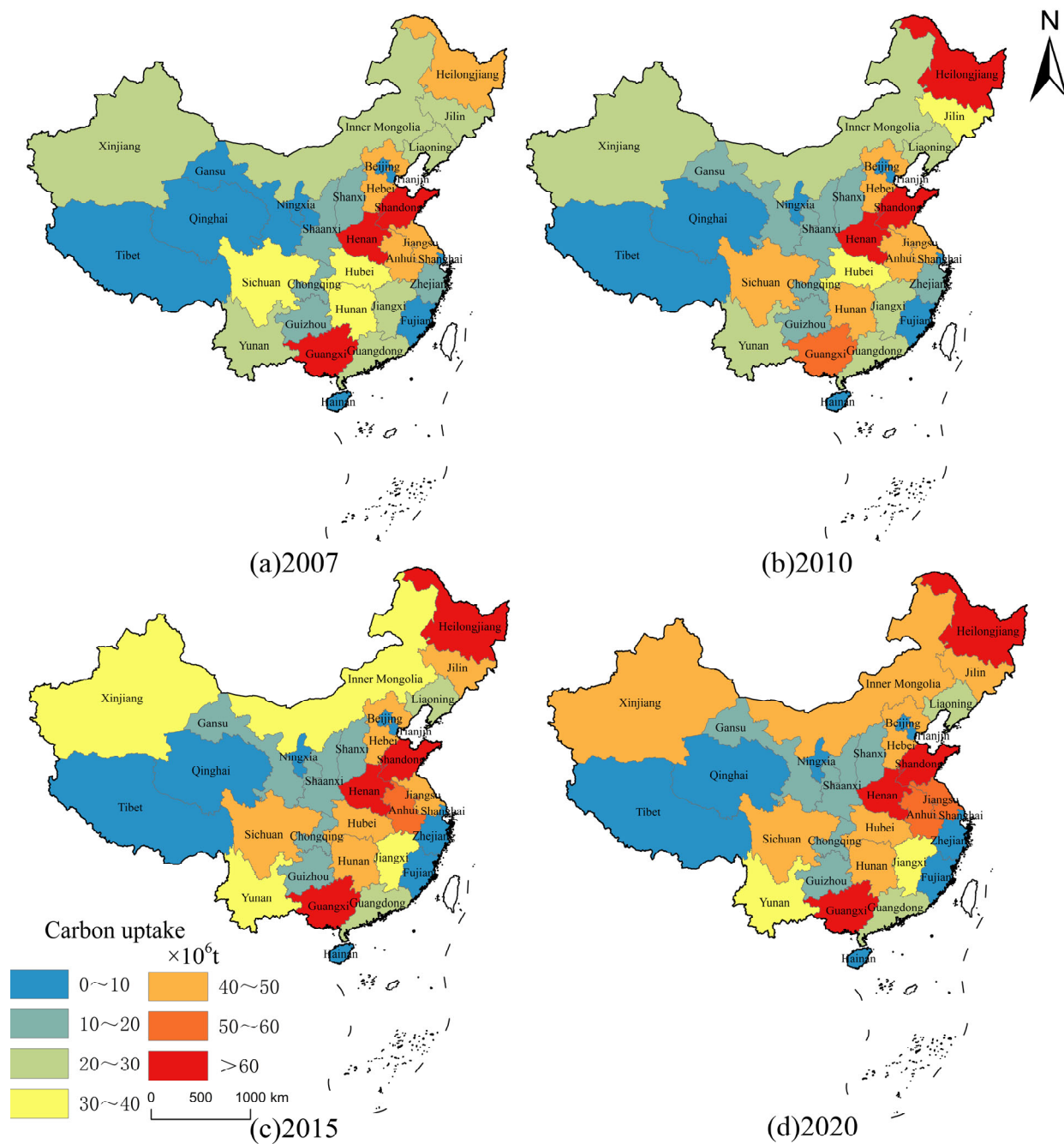
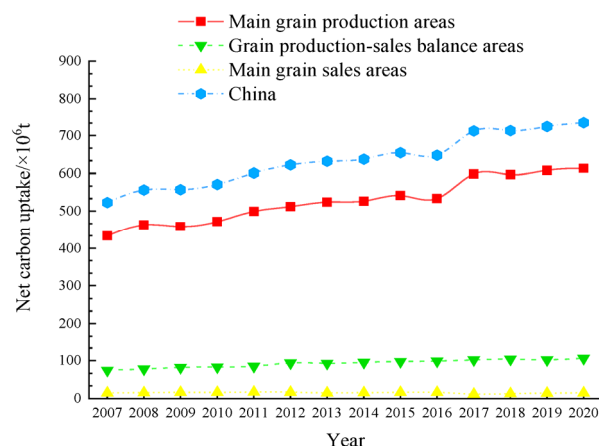


Figure 6. Evolution map of carbon uptake on China’s farmland in 2007 (a), 2010 (b), 2015 (c), and 2020 (d).



**Figure 7.** Net carbon uptake on farmland in China.

From a functional area perspective, from 2007 to 2020, except for the main grain sales areas, the net carbon uptakes in all other areas displayed an upwards trend. Obviously, the trend of net carbon uptake in the main grain production areas was similar to that of China.

From a spatial perspective (Figure 8), except for that in Guangxi and Hainan, the net carbon uptake on farmland in other provinces of China was positive, indicating that the agricultural production sector in these regions can to some extent offset some of the greenhouse gas emissions caused by secondary and tertiary industries. Among the provinces, Henan ranked first with an absolute advantage, with net carbon uptake as high as  $81.99 \times 10^6$  t, followed by Heilongjiang at  $63.27 \times 10^6$  t. The regions ranked 3rd to 10th in terms of net carbon uptakes were Shandong ( $61.52 \times 10^6$  t), Anhui ( $41.65 \times 10^6$  t), Hebei ( $39.84 \times 10^6$  t), Jiangsu ( $38.51 \times 10^6$  t), Jilin ( $35.66 \times 10^6$  t), Sichuan ( $35.54 \times 10^6$  t), Xinjiang ( $30.97 \times 10^6$  t), and Hubei ( $30.06 \times 10^6$  t). The net carbon uptake of these 10 regions accounted for 72.29% of China's total net carbon uptake. Guangxi had the lowest net carbon-uptake value at  $-13.57 \times 10^6$  t, followed by Hainan at  $-0.48 \times 10^6$  t. The regions ranked from the bottom 3rd to 9th were Tibet ( $0.38 \times 10^6$  t), Beijing ( $0.78 \times 10^6$  t), Shanghai ( $0.90 \times 10^6$  t), Qinghai ( $1.22 \times 10^6$  t), Tianjin ( $2.11 \times 10^6$  t), Fujian ( $3.00 \times 10^6$  t), and Ningxia ( $3.33 \times 10^6$  t), with a total net carbon uptake of these 9 provinces being negative. Notably, there were significant differences in net carbon uptake among 31 provinces in China, with a prominent polarization phenomenon.

### 3.4. Carbon-Emission Reduction Potential of Farmland

Due to the convergence of geographical conditions, economic interactions, and flows and transfer of factors, as well as the promotion and diffusion of production methods and technologies, regional agricultural production and operation activities affect each other. Therefore, this study refers to the study of Zhang [48], in which one benchmark was selected in advance to compare the existing carbon-emission intensity in each province with the benchmark, and then, the difference between them was the carbon-emission reduction potential. The absolute convergence method was first used to estimate the farmland carbon-emissions reduction potential of 31 provinces in China (assuming that all provinces converge to the same minimum value), and, then, the conditional convergence method was used to estimate the carbon-emissions reduction potential of the main grain production areas, grain production–sales balance areas, and main grain sales areas (assuming that all provinces converge to the lowest value in their respective functional areas).

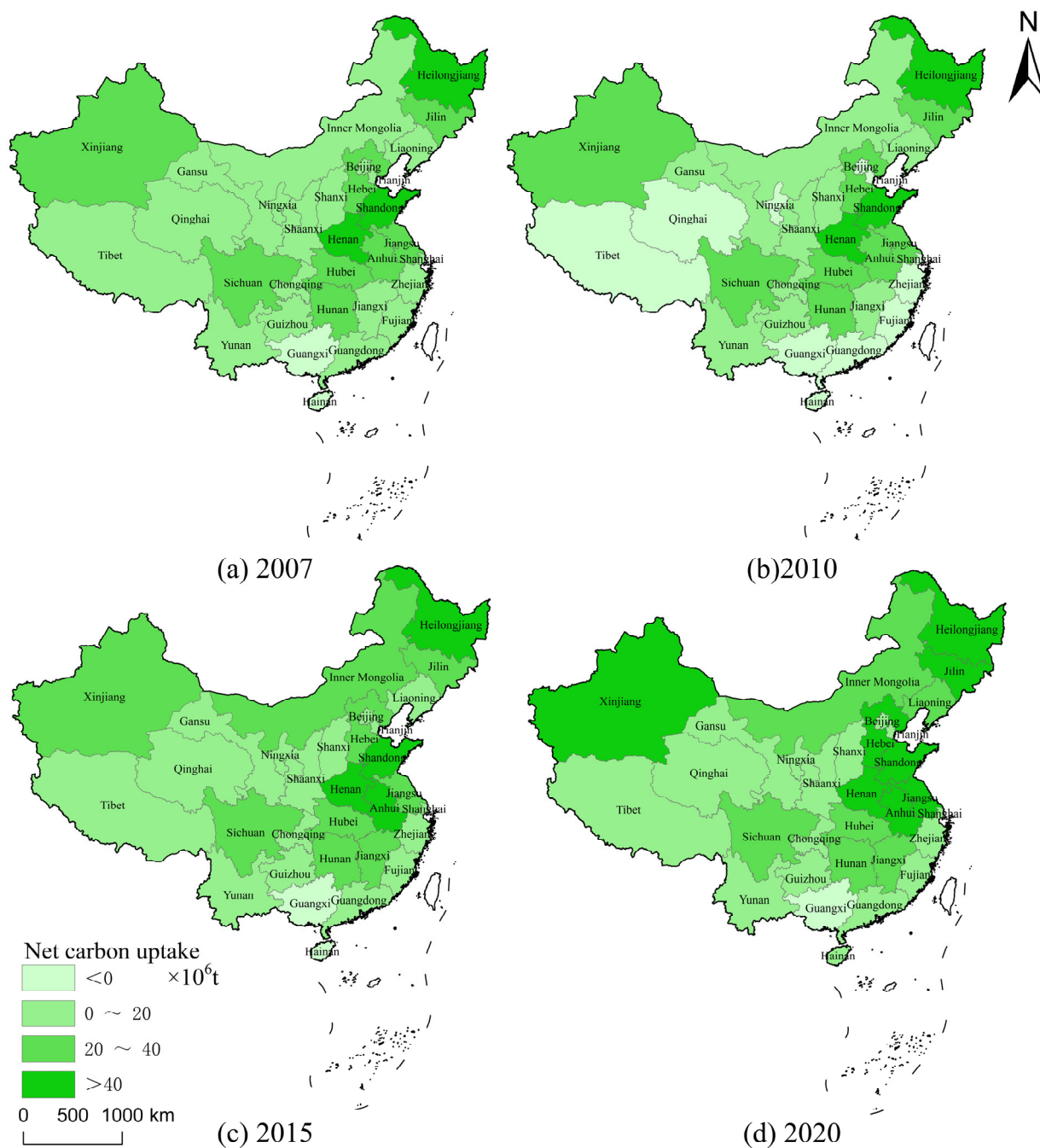


**Figure 8.** Evolution map of net carbon uptake on China's farmland in 2007 (a), 2010 (b), 2015 (c), and 2020 (d).

### 1. Potential for carbon-emission reduction on farmland at a national level

Using Beijing, which has the lowest carbon-emission intensity in the country, as a benchmark, the carbon-emissions reduction potential of 31 provinces in China was calculated, and Table 4 was obtained based on the classification criteria for carbon-emission reduction potential [49].

**Table 4.** Average carbon-emission reduction potential of farmland in 31 provinces from 2007 to 2020.

Classification	Scope	Region	Amount
Low reduction potential	≤20%	Beijing (0%), Shaanxi (16.27%), Qinghai (11.86%)	3
Medium reduction potential	20~50%	Tianjin (34.36%), Hebei (33.60%), Shanxi (30.39%), Inner Mongolia (45.72%), Liaoning (46.67%), Shandong (20.33%), Henan (30.34%), Chongqing (48.60%), Sichuan (43.03%), Tibet (30.34%), Gansu (33.26%), Xinjiang (41.32%)	12
High reduction potential	50~70%	Jilin (64.95%), Heilongjiang (63.41%), Shanghai (56.61%), Jiangsu (55.49%), Zhejiang (59.85%), Anhui (69.90%), Fujian (58.09%), Hubei (61.75%), Hunan (69.72%), Guizhou (51.12%), Ningxia (51.05%)	11
Highest reduction potential	≥70%	Jiangxi (79.75%), Guangdong (82.75%), Guangxi (96.37%), Hainan (85.20%), Yunnan (85.96%)	5

There are 28 provinces in medium and high reduction-potential areas, accounting for 90.32% of all provinces in China. This result indicates that in most provinces, the carbon-emission intensity on farmland is high, leaving substantial room for emission reduction. Sixteen provinces had a reduction potential of more than 50%, including 7 provinces in the main grain production areas, 4 provinces in the grain production–sales balance areas, and 5 provinces in the main grain sales areas. The two provinces with the lowest carbon-emission reduction potential, in addition to Beijing as a standard, were Shaanxi and Qinghai, both from the grain production–sales balance areas. Looking at the three main grain functional areas, the main grain production areas had the highest potential for carbon-emissions reduction; at the same time, the grain production–sales balance areas had the lowest potential for carbon-emissions reduction. From a nationwide perspective, there were 10 provinces with carbon-emissions reduction potential less than 45% and 21 provinces with carbon-emissions reduction potential greater than 45%, which account for 2/3 of the total and, therefore, face greater pressure to reduce emissions. This scenario may have a certain impact on grain production and ignores the differences in agricultural production conditions among regions.

## 2. Potential for carbon-emission reduction on farmland at a regional level

Table 5 provides the potential for carbon-emission reduction on farmland across 31 provinces at the regional level. It is assumed that the carbon-emission intensity of farmland in each province within the three main grain functional areas will approach the lowest level in the respective functional areas. Specifically, for provinces within the main grain production area, Shandong is taken as the standard; for provinces within the grain production–sales balance area, Qinghai is taken as the standard; and for provinces within the main grain sales area, Beijing is taken as the standard.

The carbon-emission reduction potential of the three main grain functional areas was still significant, with the greatest potential in the main grain sales area, with an average potential of 53.83% reduction. The average potential for carbon-emissions reduction in the main grain production area was 40.59%, while the potential in the grain production–sales balance area was the lowest, with an average potential of only 37.76%. In most provinces under regional convergence, the carbon-emissions reduction potential was lower than the national average (equal to the main grain sales area), indicating that the carbon-emissions reduction space in most provinces will be reduced and the pressure to reduce emissions will correspondingly decrease. Moreover, under regional convergence, the carbon-emissions reduction potential of only 13 provinces exceeded 45%, while the potentials of the other 18 provinces were less than 45%, which will also reduce the impact on grain production.

**Table 5.** Average carbon-emission reduction potential of farmland in China's three main grain functional areas from 2007 to 2020.

Main Grain Production Area		Grain Production–Sales Area		Main Grain Sales Area	
Region	Reduction Potential	Region	Reduction Potential	Region	Reduction Potential
Heilongjiang	54.07%	Shanxi	21.02%	Beijing	0.00%
Jilin	56.01%	Ningxia	44.46%	Tianjin	34.36%
Inner Mongolia	31.87%	Qinghai	0.00%	Shanghai	56.61%
Henan	12.57%	Gansu	24.27%	Zhejiang	59.85%
Jiangxi	74.59%	Tibet	20.96%	Fujian	58.09%
Anhui	62.22%	Yunnan	84.07%	Guangdong	82.75%
Hebei	16.65%	Guizhou	44.54%	Hainan	85.20%
Liaoning	33.07%	Chongqing	41.68%		
Hubei	51.99%	Guangxi	95.88%		
Hunan	62.00%	Shaanxi	5.00%		
Jiangsu	44.14%	Xinjiang	33.42%		
Shandong	0.00%				
Sichuan	28.50%				
Average	40.59%	Average	37.76%	Average	53.83%

According to the calculation results in Table 5, clustering the 31 provinces in China was completed through matrix construction. Based on the three main grain functional areas and the three levels of carbon-emission reduction potential, the 31 provinces were classified into eight types of regions, as shown in Figure 9.

	Main grain production area	Grain production–sales balance area	Main grain sales area
High ( $\geq 50\%$ )	I (Heilongjiang, Jilin, Jiangxi, Anhui, Hubei, Hunan)	II (Yunnan, Guangxi)	III (Shanghai, Zhejiang, Fujian, Guangdong, Hainan)
Medium (20%–50%)	IV (Inner Mongolia, Liaoning, Jiangsu, Shandong)	V (Shanxi, Ningxia, Gansu, Tibet, Guizhou, Chongqing, Xinjiang)	VI (Tianjin)
Low ( $\leq 20\%$ )	VII (Henan, Hebei)	VIII (Shaanxi)	

**Figure 9.** Clustering results of carbon-emission reduction potential in China.

Heilongjiang, Jilin, Jiangxi, Anhui, Hubei, and Hunan were all Category I regions. While ensuring that the total agricultural output is not affected, the promotion of maximum farmland carbon-emissions reduction should be pursued. Heilongjiang and Jilin are located in the black earth region of Northeast China, which has excellent agricultural production conditions and can promote sustainable agricultural development that is “resource-saving, environmentally friendly, and ecologically protective”. Hubei, Hunan, Jiangxi, and Anhui are located in the middle reaches of the Yangtze River, with abundant water resources and a large population. A more mature agricultural system has been developed, but it is also necessary to take full advantage of the advantages of location; promote the flow of talent, capital, and other factors; and improve the efficiency of resource allocation.

Yunnan and Guangxi were in the Category II region. Due to geographical constraints, agriculture in this region is small-scale, and soil quality is relatively poor; therefore, the carbon intensity of farmland should be moderately reduced. By strengthening agricultural production management and improving the level of agricultural modernization, this can be achieved. In addition, in this region, rice and various vegetables are planted in multiple seasons, which may result in a large amount of fertilizer being applied, while

ammonia easily evaporates under high temperature conditions. Farmers should actively use organic fertilizers, nitrogen fertilizer enhancers, and biomass charcoal to reduce soil nitrous oxide emissions.

Shanghai, Zhejiang, Fujian, Guangdong, and Hainan were in the Category III region. These provinces are economically developed, with rapid industrialization and urbanization, which have had an obvious negative impact on agricultural production. Additionally, due to high population density, the amount of arable land for agriculture has been continuously decreasing, leading to a decline in the area of farmland for grain cultivation. To address these challenges, the region should leverage its economic advantages, optimize the allocation of agricultural production resources, further reduce the proportion of traditional agriculture, and vigorously develop high-value-added agricultural sectors such as leisure agriculture and ecological agriculture to improve the multifunctionality of agricultural production.

Inner Mongolia, Liaoning, Jiangsu, and Shandong were in the Category IV region. These provinces can reduce carbon emissions by reducing agricultural inputs, such as replacing chemical fertilizers with organic fertilizers. The Category V region included Shanxi, Ningxia, Gansu, Tibet, Guizhou, Chongqing, and Xinjiang, where the soil, climate, and technology for agricultural production are relatively poor. To ensure grain production and reduce carbon emissions, the government should fully carry out its macrocontrol role, with the optimization of the agricultural industry structure as the core, scientifically plan the agricultural industry layout, and promote energy-saving and carbon-emissions reduction technologies. The carbon-emissions reduction space was relatively small in the Category VI region (Tianjin), VII region (Henan, Hebei), and VIII region (Shaanxi). In the future, it is necessary for these regions to provide training to strengthen farmers' skills, promote low-carbon planting techniques, and encourage farmers to adopt low-carbon production methods.

#### 4. Discussion

According to the Second National Climate Change Information Communication of the People's Republic of China, China's annual carbon emissions have reached the requirement of the National Development and Reform Commission ( $7.22 \times 10^{12}$  kg) [50]. In previous studies, the decreasing trend in China's agricultural carbon emissions has been fully recognized [2]. This study found that China's farmland carbon emissions displayed a fluctuating downwards trend from 2007 to 2020. The reason for this trend may be due to the issuance and implementation of the No. 1 Central Document in 2008, which initiated control of the carbon emissions of the planting industry at the policy level. On the other hand, the document proposed actively developing rice production and accelerating the promotion of agricultural mechanization, which may have increased the emissions of  $\text{CH}_4$  and  $\text{CO}_2$ . In addition, in 2015, the Ministry of Agriculture issued the "Zero Growth Action Plan for Fertilizer Use by 2020" and the "Zero Growth Action Plan for Pesticide Use by 2020," and, in 2016, the State Council issued the "13th Five-Year Plan for Controlling Greenhouse Gas Emissions". The implementation of these policies greatly reduced  $\text{CO}_2$  and  $\text{N}_2\text{O}$  emissions [37]. The results of this study show that the carbon-emission intensity of China's farmland exhibits certain clustering characteristics in space, which is consistent with the results of Pang [51]. This study indicates that the carbon-emission intensity of China's farmland exhibits a "north cold and south hot" spatial pattern. For climatic reasons, single-season rice is grown in northern China. However, in the central and southern regions of China, double-season rice is grown at a high density [52]. In addition,  $\text{CH}_4$  emission factors are higher in rice fields in southern China than in northern China, resulting in higher  $\text{CH}_4$  emissions in southern China. Furthermore, in China, the application of synthetic nitrogen fertilizer on crops is approximately two to three times that in developed countries [53]. In addition, China mainly relies on coal as a raw material for production, indicating that China's fertilizer production has high energy consumption and low utilization efficiency [54]. The hot weather in southern China makes it easy for

ammonia in fertilizer to volatilize under high-temperature conditions. At the same time, the increasing trend of  $N_2O$  is 298 times that of  $CO_2$  and 11.92 times that of  $CH_4$ , which also explains why  $N_2O$  emissions account for the largest proportion of total carbon emissions.

The carbon-uptake structure of Chinese farmland is relatively stable, with rice, maize, and wheat being the main sources of agricultural carbon uptake, accounting for approximately 80% together, which is consistent with the results of Chen [55]. It is worth noting that although the planting area of economic crops in China has increased significantly in recent years and the yield has also steadily increased, the dominance of grain crops has not changed, making grain crops the main source of carbon uptake on farmland. There are significant spatial differences in carbon uptake in Chinese farmland. The reason for this is that China is a vast country, and agricultural production varies greatly from region to region, with different crops suitable for cultivation and different crops having different carbon-uptake capacities, leading to variations in crop carbon storage. The results of this study show that from 2007 to 2020, the amount of carbon uptake on farmland was higher than the amount of carbon emissions, indicating that farmland had a carbon-uptake effect. This finding is similar to the results of Tian [56] and Cui [57]. The carbon emissions, carbon uptake, and net carbon uptake derived from this study are different from those of other studies, mainly for three reasons. First, different carbon sources were considered. This study considered 10 carbon-emission sources, which were nitrogen leaching runoff, atmospheric nitrogen deposition, straw returning, fertilizer application, rice planting, farmland irrigation, farmland ploughing, agricultural machinery, pesticide use, and plastic film use, when calculating carbon emissions from farmland. This approach is different from that in Tian [58] and Wang [43]. Second, the calculation of farmland carbon uptake considered the coefficient of water. In the estimation of crop carbon uptake, crop biomass is often calculated using crop yield data, but the crop yield in statistical data does not refer to the dry weight of the harvested part (fruit) of the crop. The water content of the harvested part of the crop should be considered when conducting estimations, and this approach is different from that in Chen [59]. Third, many coefficients were applied in the calculation. The carbon-emission coefficient and crop coefficient in different studies are also different.

Due to the limited availability of data, this study only considered the carbon uptake of crops when estimating the amount of carbon uptake on farmland and did not estimate the carbon stored in soils, which, to some extent, affected the accuracy of the calculations. Second, only 13 major crops were selected when calculating the carbon effect of farmland, and not all crops were included in the calculation. Furthermore, the selection of carbon-emission coefficients was based on relevant domestic and international literature, which may not be entirely applicable to the calculation of farmland carbon emissions in different provinces of China. Therefore, further improvement and revision are needed in future research. In addition, when estimating the carbon-emission reduction potential in different provinces of China, only the differences between the three main grain functional areas in China were considered, and the differences within each functional area were not fully taken into account. The potential for carbon-emission reduction on farmland needs to be further explored in subsequent studies. Finally, the carbon effect on farmland is a complex issue and we will have to continue to refine our analytical models in the future to provide policy recommendations for the low-carbon development of agriculture in China.

## 5. Conclusions

Based on agricultural statistical data from 31 provinces in China from 2007 to 2020, this study explored the spatial-temporal evolution characteristics of carbon emissions, carbon uptake, and net carbon uptake on Chinese farmland using the life cycle assessment method and spatial autocorrelation analysis method. The carbon-emission reduction potential of farmland in China was estimated. The following research conclusions were obtained from this research:

1. From 2007 to 2020, the carbon emissions from farmland in China displayed a fluctuating downwards trend, with the highest carbon emissions in 2013 at approximately  $9.4665 \times 10^8$  t. The carbon-emission intensity displayed a downwards trend, from 0.35 kg/CNY in 2007 to 0.12 kg/CNY in 2020, exhibiting a “cold north and hot south” spatial pattern;
2. The carbon uptake on farmland in China displayed an overall upwards trend during the study period, increasing by 27.73% compared to that in 2007. Rice, maize, and wheat were the main sources of carbon uptake, and high-carbon-uptake areas were mainly distributed in eastern China; conversely, low-carbon-uptake areas were mainly distributed in southwest China;
3. Over the 14 years, net carbon uptake was the main feature of Chinese farmland and increased from  $522.81 \times 10^6$  t in 2007 to  $734.50 \times 10^6$  t in 2020. At the same time, there were significant differences in net carbon uptake among 31 provinces in China, with a prominent polarization phenomenon;
4. China has a great potential to reduce carbon emissions from farmland, with the average carbon-emission reduction potentials from high to low in main grain sales areas, main production areas, and grain production–sales balance areas being 53.83%, 40.59%, and 37.76%, respectively.

This study helps clarify the current situation and evolutionary trend of the carbon effect on Chinese farmland, providing a reference and solutions for decision making on the “dual-carbon” strategy and helping to achieve the goal of “dual-carbon” in agriculture.

**Author Contributions:** Y.W. performed the statistical analysis, wrote this manuscript, and revised this manuscript. J.Y. was responsible for data visualization, wrote this manuscript, and revised this manuscript. C.D. revised this manuscript. All authors have read and agreed to the published version of the manuscript.

**Funding:** This study was supported by the Open Project of the Key Laboratory of Combining Farming and Animal Husbandry, the Ministry of Agriculture and Rural Affairs; and the China Postdoctoral Science Foundation (2022MD713723).

**Institutional Review Board Statement:** Not applicable.

**Informed Consent Statement:** Not applicable.

**Data Availability Statement:** The data that support the findings of this study are available from the corresponding author upon reasonable request.

**Conflicts of Interest:** The authors declare no conflict of interest.

## References

1. Xiao, G.J.; Zhang, Q. Impact of global climate change on agro-ecosystem: A review. *Chin. J. Appl. Ecol.* **2007**, *18*, 1877–1885.
2. Yang, H.; Wang, X.; Peng, B. Agriculture carbon-emission reduction and changing factors behind agricultural eco-efficiency growth in China. *J. Clean. Prod.* **2022**, *334*, 130193. [CrossRef]
3. IPCC. Climate Change 2021: The Physical Science Basis. Working Group I Contribution to the Sixth Assessment Report of the Intergovernmental Panel on Climate Change. 2022. Available online: <https://www.ipcc.ch/report/ar6/wg1/#fullreport> (accessed on 14 April 2023).
4. Zheng, B.F.; Liang, H.; Wan, W.; Liu, Z.; Zhu, J.Q.; Wu, Z.J. Spatial-temporal pattern and influencing factors of agricultural carbon emissions at the county level in Jiangxi Province of China. *Trans. CSAE* **2022**, *38*, 70–80.
5. Zeng, X.G.; Yu, C. Studies on carbon emission structure and carbon peak of agriculture and rural areas in China. *China Environ.* **2022**, *in press*.
6. Luo, H.L. Advances on carbon storage in crops of China. *Ecol. Environ. Sci.* **2014**, *23*, 692–697.
7. Luo, H.L. Dynamic of Vegetation Carbon Storage of Farm land Ecosystem in Hilly Area of Central Sichuan Basin during the Last 55 Years—A Case of Yanting Country, Sichuan Province. *J. Nat. Resour.* **2009**, *24*, 251–258.
8. Jiang, Q.O.; Deng, X.Z.; Zhan, J.Y.; Liu, X.Q. Impacts of cultivated land conversion on the vegetation carbon storage in the Huang–Huai–Hai Plain. *Geogr. Res.* **2008**, *27*, 839–847.
9. Gao, Z.Q.; Liu, J.Y. A comparative study of the net productivity of vegetation in China. *Chin. Sci. Bull.* **2008**, *53*, 317–326.
10. Zhao, M.Y.; Liu, Y.X.; Zhang, X.Y. A review of research advances on carbon sinks in farmland ecosystem. *Acta Ecol. Sin.* **2022**, *42*, 9405–9416.

11. Dioha, M.O.; Kumar, A. Exploring greenhouse gas mitigation strategies for agriculture in Africa: The case of Nigeria. *AMBIO J. Hum. Environ.* **2020**, *49*, 1549–1566. [[CrossRef](#)]
12. Hemingway, C.; Vigne, M.; Aubron, C. Agricultural greenhouse gas emissions of an Indian village—Who’s to blame: Crops or livestock? *Sci. Total Environ.* **2023**, *856*, 159145. [[CrossRef](#)]
13. Li, M.Q.; Liu, S.L.; Sun, Y.X.; Liu, Y.X. Agriculture and animal husbandry increased carbon footprint on the Qinghai-Tibet Plateau during past three decades. *J. Clean. Prod.* **2021**, *278*, 123963. [[CrossRef](#)]
14. Dyer, J.A.; Desjardins, R.L. Energy based GHG emissions from Canadian agriculture. *J. Energy Inst.* **2007**, *80*, 93–95. [[CrossRef](#)]
15. Yan, M.; Luo, T.; Bian, R.; Cheng, K.; Pan, G.; Rees, R. A comparative study on carbon footprint of rice production between household and aggregated farms from Jiangxi, China. *Environ. Monit. Assess.* **2015**, *187*, 332.1–332.11. [[CrossRef](#)]
16. Platis, D.P.; Anagnostopoulos, C.D.; Tsaoulas, A.D.; Meneses, G.C.; Kalburtji, K.L.; Mamolos, A.P. Energy Analysis, and Carbon and Water Footprint for Environmentally Friendly Farming Practices in Agroecosystems and Agroforestry. *Sustainability* **2019**, *11*, 1664. [[CrossRef](#)]
17. Haider, A.; Bashir, A.; Husnain, M. Impact of agricultural land use and economic growth on nitrous oxide emissions: Evidence from developed and developing countries. *Sci. Total Environ.* **2020**, *741*, 140421. [[CrossRef](#)] [[PubMed](#)]
18. Shah, A.N.; Iqbal, J.; Tanveer, M.; Yang, G.Z.; Hassan, W.; Fahad, S.; Yousaf, M.; Wu, Y.Y. Nitrogen fertilization and conservation tillage: A review on growth, yield, and greenhouse gas emissions in cotton. *Environ. Sci. Pollut. Res.* **2016**, *24*, 2261–2272. [[CrossRef](#)]
19. Li, M.; Li, H.; Fu, Q.; Liu, D.; Yu, L.; Li, T. Approach for optimizing the water-land-food-energy nexus in agroforestry. *Agric. Syst.* **2021**, *192*, 103201. [[CrossRef](#)]
20. Winiwarter, W.; Leip, A.; Tuomisto, H.L.; Hastrup, P. A European perspective of innovations towards mitigation of nitrogen-related greenhouse gases. *Curr. Opin. Environ. Sustain.* **2014**, *9–10*, 37–45. [[CrossRef](#)]
21. Hu, N.J.; Shi, H.; Zhu, L.Q. Effect of different straw returning modes on carbon footprint in a rice-wheat rotation system. *Resour. Environ. Yangtze Basin* **2018**, *27*, 2775–2783.
22. Ismael, M.; Srouji, F.; Boutabba, M.A. Agricultural technologies and carbon emissions: Evidence from Jordanian economy. *Environ. Sci. Pollut. Res.* **2018**, *25*, 10867–10877. [[CrossRef](#)]
23. Adenaeuer, L.; Breen, J.; Witzke, P.; Kesting, M.; Hayden, A.; Donnellan, T. The potential impacts of an EU-wide agricultural mitigation target on the Irish agriculture sector. *Clim. Policy* **2023**, *23*, 495–508. [[CrossRef](#)]
24. Huang, J.; Sun, Z.; Zhong, P. The Spatial Disequilibrium and Dynamic Evolution of the Net Agriculture Carbon Effect in China. *Sustainability* **2022**, *14*, 13975. [[CrossRef](#)]
25. Lin, C.C.; He, R.X.; Liu, W.Y. Considering Multiple Factors to Forecast CO<sub>2</sub> Emissions: A Hybrid Multivariable Grey Forecasting and Genetic Programming Approach. *Energies* **2018**, *11*, 3432. [[CrossRef](#)]
26. Rehman, E.; Ikram, M.; Rehman, S.; Feng, M.T. Growing green? Sectoral-based prediction of GHG emission in Pakistan: A novel NDGM and doubling time model approach. *Environ. Dev. Sustain.* **2021**, *8*, 23. [[CrossRef](#)]
27. Abbas, N.A.; Hamrani, A.; Madramootoo, C.A.; Zhang, T.Q.; Tan, C.S.; Goyal, M.K. Modelling carbon dioxide emissions under a maize-soy rotation using machine learning. *Biosyst. Eng.* **2021**, *212*, 1–18. [[CrossRef](#)]
28. Kolasa-Wiecek, A. Neural Modeling of Greenhouse Gas Emission from Agriculture Sector in European Union Member Countries. *Water Air Soil Pollut.* **2018**, *229*, 205.1–205.12. [[CrossRef](#)]
29. Li, Y.; Chen, M.P. Analysis of influencing factors and peak forecast of non-CO<sub>2</sub> greenhouse gas emissions from provincial agricultural sources in China. *Acta Sci. Circumstantiae* **2021**, *41*, 5174–5189.
30. Yang, F.; Han, Y.H.; Wei, X.; Bi, H.T.; Wang, X.Y. Estimation of Agricultural Greenhouse Gas Emissions and Emission Reduction Potential of Beijing During the “14th Five-Year Plan” Period Under the Background of “Carbon Peak and Neutrality”. *Environ. Sci.* **2022**, *in press*.
31. Cai, Y.R.; Wang, L.G. Carbon sequestration and greenhouse gas mitigation paths and modes in a typical agroecosystem in northern China. *Chin. J. Eco-Agric.* **2022**, *30*, 641–650.
32. Blace, A.; Cuka, A.; Siljkovic, Z. How dynamic is organic? Spatial analysis of adopting new trends in Croatian agriculture. *Land Use Policy* **2020**, *99*, 105036. [[CrossRef](#)]
33. Blanco-Canqui, H. No-till technology has limited potential to store carbon: How can we enhance such potential? How dynamic is organic? *Agric. Ecosyst. Environ.* **2021**, *313*, 107352. [[CrossRef](#)]
34. Singh, H.; Northup, B.K.; Baath, G.S.; Gowda, P.P.; Kakani, V.G. Greenhouse mitigation strategies for agronomic and grazing lands of the US Southern Great Plains. *Mitig. Adapt. Strateg. Glob. Chang.* **2020**, *25*, 819–853. [[CrossRef](#)]
35. Ntiamoah, E.B.; Appiah-Otoo, I.; Li, D.; Twumasi, M.A.; Yeboah, E.N.; Chandio, A.A. Estimating and mitigating greenhouse gas emissions from agriculture in West Africa: Does threshold matter? *Environ. Dev. Sustain.* **2023**; *in press*. [[CrossRef](#)]
36. Chen, M.P.; Chen, Y.R.; Jiang, S.; Forsell, N. Toward carbon neutrality before 2060: Trajectory and technical mitigation potential of non-CO<sub>2</sub> greenhouse gas emissions from Chinese agriculture. *J. Clean. Prod.* **2022**, *368*, 133186. [[CrossRef](#)]
37. Wang, Y.; Yang, J.; Wang, J.L. Spatial-temporal pattern and trend analysis of carbon emission from farmland ecosystem. *J. China Agric. Univ.* **2023**, *28*, 89–101.
38. IPCC. Climate Change 2021: Change 2013-The Physical Science Basis Working Group I Contribution to the Fifth Assessment Report of the Intergovernmental Panel on Climate Change. 2014. Available online: <https://www.ipcc.ch/report/ar5/wg1/> (accessed on 14 April 2023).

39. West, T.O.; Marland, G. A synthesis of carbon sequestration, carbon emissions, and net carbon flux in agriculture: Comparing tillage practices in the United States. *Agric. Ecosyst. Environ.* **2002**, *91*, 217–232. [[CrossRef](#)]
40. Wu, F.L.; Li, L.; Zhang, H.L.; Chen, F. Effects of conservation tillage on net carbon flux from farmland ecosystems. *Chin. J. Ecol.* **2007**, *26*, 2035–2039.
41. Chen, X.; Shuai, C.; Wu, Y.; Zhang, Y. Analysis on the carbon emission peaks of China's industrial, building, transport, and agricultural sectors. *Sci. Total Environ.* **2020**, *709*, 135768. [[CrossRef](#)]
42. Zhang, L.; Pang, J.; Chen, X.; Lu, Z. Carbon emissions, energy consumption and economic growth: Evidence from the agricultural sector of China's main grain-producing areas. *Sci. Total Environ.* **2019**, *665*, 10–1025. [[CrossRef](#)]
43. Wang, G.F.; Liao, M.L.; Jiang, J. Research on Agricultural Carbon Emissions and Regional Carbon Emissions Reduction Strategies in China. *Sustainability* **2020**, *12*, 2627. [[CrossRef](#)]
44. Gu, J.C.; Zha, L.S. Research on dynamic change of vegetation carbon storage of crops in the Wan Jiang city belt. *Resour. Environ. Yangtze Basin* **2012**, *21*, 1507–1513.
45. Weng, L.Y.; Zhu, Z.Y.; Han, X.G.; Tan, J.Z. Spatial-temporal pattern of net carbon sink of farmland vegetation in Jiangsu Province. *Trans. CSAE* **2018**, *34*, 233–241.
46. Cheng, Y.Q.; Wang, Z.Y.; Ye, X.Y.; Wei, Y.H. Spatiotemporal dynamics of carbon intensity from energy consumption in China. *J. Geogr. Sci.* **2014**, *24*, 631–650. [[CrossRef](#)]
47. Wang, X.X.; He, A.Z.; Zhao, J. Regional disparity and dynamic evolution of carbon emission reduction maturity in China's service industry. *J. Clean. Prod.* **2020**, *244*, 118926. [[CrossRef](#)]
48. Zhang, J.W.; Zhang, J.H.; Wu, F.W. Analysis of carbon emissions from grain production and the pathways to reduce them in China. *Stat. Decis.* **2018**, *34*, 168–172.
49. Wang, L.F.; Duan, W.J.; Lai, M.Y.; Liu, L.J. Study on the regional differences and industry differences of energy-saving potentiality in China's manufacturing industry. *Geogr. Res.* **2015**, *34*, 109–121.
50. Zhang, G.; Wang, X.K.; Zhang, L.; Xiong, K.N.; Zheng, C.Y.; Lu, F.; Zhao, H.; Zheng, H.; Ouyang, Z.Y. Carbon and water footprints of major cereal crops production in China. *J. Clean. Prod.* **2018**, *194*, 613–623. [[CrossRef](#)]
51. Pang, J.X.; Li, H.J.; Lu, C.P.; Lu, C.Y.; Chen, X.P. Regional differences and dynamic evolution of carbon emission intensity of agriculture production in China. *Int. J. Environ. Res. Publ. Health* **2020**, *17*, 7541. [[CrossRef](#)]
52. Wang, W.; Guo, L.P.; Li, Y.C.; Su, M.; Lin, Y.B.; Christian, D.P.; Ju, X.T.; Lin, E.D.; Dominic, M. Greenhouse gas intensity of three main crops and implications for low-carbon agriculture in China. *Clim. Chang.* **2015**, *128*, 57–70. [[CrossRef](#)]
53. Chen, Z.D.; Xu, C.C.; Li, Y.C.; Ji, L.; Feng, J.F.; Li, F.B.; Zhou, X.Y.; Fang, F.P. Effects of multi-cropping system on temporal and spatial distribution of carbon and nitrogen footprint of major crops in China. *Glob. Ecol. Conserv.* **2019**, *22*, e00895. [[CrossRef](#)]
54. Liu, W.W.; Zhang, G.; Wang, X.K.; Lu, F.; Ouyang, Z.Y. Carbon footprint of main crop production in China: Magnitude, spatial-temporal pattern and attribution. *Sci. Total Environ.* **2018**, *654*, 1296–1308. [[CrossRef](#)] [[PubMed](#)]
55. Chen, L.Y.; Xue, L.; Xue, Y. Spatial-temporal Characteristics of China's Agricultural Net Carbon Sink. *J. Nat. Resour.* **2016**, *31*, 596–607.
56. Tian, Y.; Zhang, J.B. Spatial-temporal Regional Differentiation Research on Net Carbon Effect of Agricultural Production in China. *J. Nat. Resour.* **2013**, *28*, 1298–1309.
57. Cui, Y.; Khan, S.U.; Sauer, J.; Zhao, M.J. Exploring the spatiotemporal heterogeneity and influencing factors of agricultural carbon footprint and carbon footprint intensity: Embodying carbon sink effect. *Sci. Total Environ.* **2022**, *846*, 157507. [[CrossRef](#)]
58. Tian, P.P.; Li, D.; Lu, H.W.; Feng, S.S.; Nie, Q.W. Trends, distribution, and impact factors of carbon footprints of main grains production in China. *J. Clean. Prod.* **2021**, *278*, 123347. [[CrossRef](#)]
59. Chen, Y.; Li, S.C.; Shui, W.; Kang, Y.H. Research on carbon footprint of agricultural ecosystem in southwest China based on EKC model. *J. Agrotech. Econ.* **2013**, *2*, 120–128.

**Disclaimer/Publisher's Note:** The statements, opinions and data contained in all publications are solely those of the individual author(s) and contributor(s) and not of MDPI and/or the editor(s). MDPI and/or the editor(s) disclaim responsibility for any injury to people or property resulting from any ideas, methods, instructions or products referred to in the content.